ChemComm

Kinetic investigation of chemical process in single-molecule junction

Journal:	*ChemComm*
Manuscript ID	CC-COM-10-2019-008383
Article Type:	Communication

COMMUNICATION

Kinetic investigation of chemical process in single-molecule junction

Received 00th January 20xx,
Accepted 00th January 20xx

DOI: 10.1039/x0xx00000x

Yusuke Hasegawa,[a] Takanori Harashima,[a] Yuki Jono,[a] Takumi Seki,[a] Manabu Kiguchi[a] and Tomoaki Nishino*[a]

We report on the kinetic investigation for the breakdown of single-molecule junctions. Currents through the junctions was measured as a function of time to elucidate their lifetimes. The analysis of the lifetimes revealed that the breakdown reaction obeys first-order reaction kinetics, and the rate constants determined from the analysis was found to reflect the stability of the junctions.

Recent advances in analytical methodologies have offered a reliable means to directly explore a single molecule and related phenomena.[1-6] Such studies contribute to realization of molecular electronics, where single molecules are utilized as electronic components,[7-10] from an application perspective. The single-molecule investigation also deepens understandings so as to bring new insights of the mechanism into a chemical reaction[11] from a fundamental viewpoint. A single-molecule junction created by bridging a single target molecule within a metal nanogap has been widely utilized to investigate single molecules.[2, 12-14] Much effort has been devoted with the single-molecule junctions to gaining the understanding of charge transport properties toward molecular electronics applications.[15] Consequently, a variety of functionalities, such as diode[16-18] and transistor effects,[19, 20] was obtained with single molecules. Although a large body of research based on the single-molecule junction has been related to the single-molecule devices, chemical transformation of the constituent molecule of the junction can be detected. For example, photo- and thermal reactions of azulene derivatives were investigated.[21] The conductances of single-molecule junctions formed by the reactant and the product molecules differ from each other by more than an order of magnitude and thereby enable the discrimination of the two chemical species. The ratio of the formed product to the remaining reactant was successfully obtained based on the conductance measurements on the single-molecule basis during the time course of the reaction. It was found that the product ratio observed within the junction deviates from the ratio measured in a solution. This and other studies[22] demonstrate that a single-molecule junction provides not only a unique way to observe a chemical reaction at the single-molecule level but also a novel opportunity to control the reaction.

Break-junction (BJ) techniques have been primarily employed to measure conductance of the single-molecule junction. Metal atomic contacts are repeatedly formed and broken down in the measurements, and a sample molecule bridges the nanogap created immediately after the breakdown of the metal contact. Alternatively, the single-molecule junction can be formed and interrogated in the time domain, i.e., via current–time (*I*–*t*) measurement.[23, 24] In this technique, a single molecule on a metal surface spontaneously and reversibly forms the molecular junction. The measurements involve no mechanical movement of the electrode unlike the BJ technique, and consequently molecular junction undergoes chemical processes, including its formation and break-down, under an equilibrium condition. It is, therefore, expected that this measurement fulfils the requirements for the kinetic and thermodynamic analyses of a chemical reaction of a single molecule, which leads to the detailed understanding of the reaction mechanisms. To this end, in the present study we investigated the breakdown process of a single-molecule junction, which can be regarded as a unimolecular decomposition reaction, based on the *I*–*t* measurement using scanning tunneling microscope (STM) and performed the kinetic analysis of the resulting current traces. It was revealed that the breakdown process obeys first-order reaction kinetics. In addition, the rate constants of the process were found to reflect the binding energy, i.e., the stability of the molecular junction. These results demonstrate that the kinetic analyses bring detailed knowledge of a chemical reaction for a single molecule.

[a] *Department of Chemistry, School of Science, Tokyo Institute of Technology, Ookayama, Meguro-ku, Tokyo 152-8551, Japan. E-mail: tnishino@chem.titech.ac.jp*

†Electronic Supplementary Information (ESI) available: Details and verification of ATA, additional histograms and experimental procedures. See DOI: 10.1039/x0xx00000x

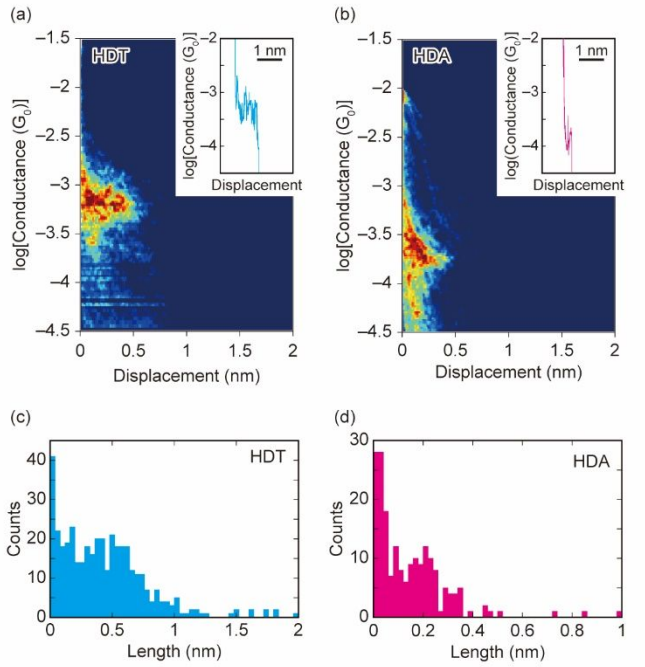

Fig. 1 2D conductance histograms and plateau length histograms for (a, c) HDT, and (b, d) HDA from STM-BJ experiments. Bias voltage, 0.1 V. 1506 and 1998 traces were analysed to construct the histograms for HDT and HDA, respectively.

In the present study, α,ω-disubstituted alkanes were employed as sample to form single-molecule junctions (see ESI† for the experimental procedures). First, to determine the conductance of the single-molecule junctions, measurements based on the STM-BJ technique were carried out. A gold STM tip was repeatedly brought into and out of contact with the gold substrate modified with the sample molecule. The conductance, calculated from the tunneling current, was recorded as a function of the tip displacement during the breakdown procedure, and Fig. 1a and 1b show the resulting two-dimensional (2D) conductance traces for 1,6-hexanedithiol (HDT) and 1,6-hexanediamine (HDA), respectively. Each histogram exhibited a clear plateau, where the conductance remains constant regardless of the increased tip–substrate distance. The plateaus indicate the formation of the single-molecule junction by the chemisorption of the terminal functional groups, i.e., -SH (HDT) or -NH_2 (HDA), to the STM tip and substrate.[12] Thus, the conductance at which the plateau appeared in the 2D histogram corresponds to the statistically most probable conductance of the single-molecule junctions. The conductance for the HDT and HDA junctions were determined to be 5.0×10^{-4} and 1.6×10^{-4} G_0, respectively, both of which are in agreement with literature.[25, 26] The rupture length, for which a single-molecule junction persists against the tip displacement, can be deduced from the conductance traces. Most of the HDT and HDA junctions rupture at approximately 0.5 and 0.2 nm, respectively, as shown in Fig. 1c and 1d. The differences in the rupture length most probably arise from the different binding energies of the analyte molecule to the gold electrodes given the variations in the terminal functional groups and the common aliphatic chain of the sample molecules.[27] Extensive investigations have been conducted to clarify thermodynamic stability of the single-molecule junctions by the STM-BJ and mechanically-controlled (MC) BJ techniques.[28-32] The resulting stability reflects kinetic properties of the target junction under forces exerted by the mechanical displacements in the BJ measurements[11] and has provided the basis for developing single-molecule electronic devices. In contrast, in the present study we focused on the stability of a single molecule without the exerted forces. Such measurements could reveal kinetic properties intrinsic to the target molecule bearing a close relationship to its chemical behavior on the surface.

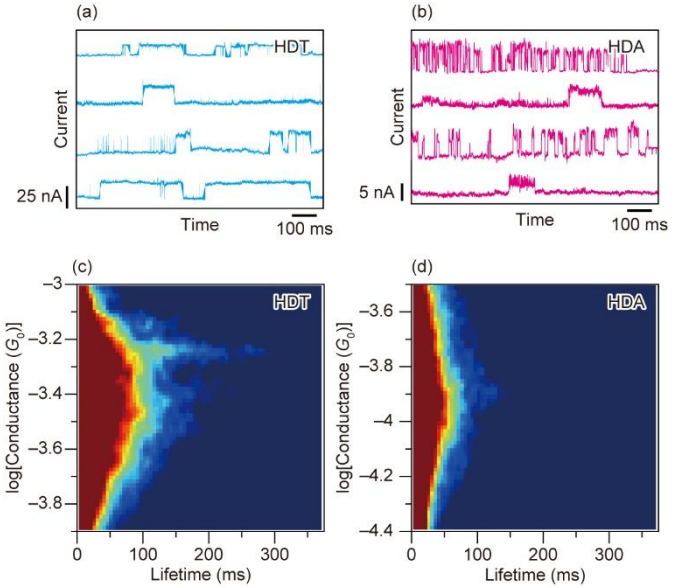

Fig. 2 Typical *I–t* traces and 2D histograms of *I–t* plateaus for (a, c) HDT, and (b, d) HDA from *I–t* experiments. Bias voltage, 0.4 V. The 2D histograms in (c) and (d) contains 22539 and 26958 plateaus, respectively.

The formation and break-down of the single-molecule junctions were detected at room temperature in the time domain by the *I–t* measurements. Unlike in the STM-BJ measurements described above, the tunneling current was recorded while the tip was held stationary in the intimate proximity to the substrate surface with the STM feedback control disabled. These measurements involve no tip displacement and thus avoid applying the external mechanical force to the molecular junctions, which leads to the expectation that the *I–t* measurement facilitates the thermodynamic analysis of single-molecule junctions. This STM *I–t* measurement bears a resemblance to an MCBJ measurement with a fixed gap.[28, 29, 33, 34] The former method has an advantage to precisely tune the gap width under the STM feedback control, while more stable molecular junctions can be formed in the latter technique. Figure 2a and 2b show the resulting current traces obtained at room temperature with the HDT and HDA samples, respectively. The steep increase in the current with accompanying plateaus repeatedly appeared in both cases. These current increases are attributed to the formation of the molecular junctions where the HDT or HDA molecule on the substrate spontaneously binds to the STM tip via its terminal thiolate or amine group.[23, 24] Hence, the conductance of the molecular junctions can be calculated on the basis of the increase current values of the plateaus. Accurate collection of

large number of plateaus is necessary for kinetic investigation. The plateaus were then extracted from each trace based on the adaptive threshold analysis,[35] which enables an automated analysis of the large datasets in an unbiased manner. The analysis utilizes threshold values recursively defined by the local averages and standard deviations of the current in the *I*–*t* traces (see Supporting Information for the detailed description). It was verified that the plateaus can be correctly detected by the ATA (Fig. S1 in the ESI†). 2D histograms were then constructed by overlaying the extracted plateaus by setting the origin of the time axis of the histograms to the point at which the current steeply increased (Fig. 2c and 2d for HDT and HDA, respectively). The conductance was determined to be 2.9×10^{-4} and 1.0×10^{-4} G_0 for HDT and HDA, respectively, based on these histograms (see also Fig. S2 in the ESI† for one-dimensional conductance histograms). These values reasonably agree with those found in the STM-BJ measurements, supporting that the *I*–*t* measurement detects the formation of the single-molecule junctions. Slight differences were noticed in the single-molecule conductance values between the BJ and *I*–*t* techniques. These are attributed to the background tunneling currents: the background currents were subtracted in the determination of the conductance in the *I*–*t* measurements (see above), while these currents were uncorrected in the case of BJ measurements.

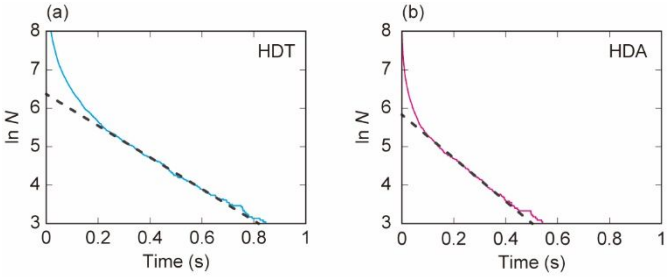

Fig. 3 Cumulative histograms for (a) HDT and (b) HDA constructed based on the lifetime of junctions observed in *I*–*t* experiments. The total number of the junctions, *N*, were plotted against time.

Current traces obtained from *I*–*t* measurements can be used to deduce lifetimes of single-molecule junctions.[33, 34, 36-38] Figure 2c and 2d shows that many junctions broke down within approximately 100 ms for HDT, while they ruptured within 50 ms in the case of HDA. These lifetimes are dominated by the kinetic properties of the single-molecule junctions, given the fact that no external force was exerted in the measurements. For quantitative analysis, the cumulative histograms of the lifetime were constructed by plotting the total number of the persisting junctions, *N*, against time in a semi-logarithmic scale (Fig. 3). All the histograms show linear regions, which means that the survival number of the single-molecule junction exponentially decays. The exponential dependence indicates the first-order kinetics of the breakdown process of the single-molecule junction. To reinforce the findings, another sample, adiponitrile (ADN) with two terminal nitrile groups, was tested, and the linear region as found in Fig. 3 emerged in the cumulative histogram (Fig. S3 in the ESI†). These results are reasonable given that the breakdown process can be regarded as the unimolecular decomposition reaction. The rate equation, $N \propto \exp(-kt)$, was used to fit the linear region in the cumulative histogram, and the rate constant *k* was determined. The single molecule junction of HDT exhibited the smallest rate constant ($3.8\ s^{-1}$), followed by those of ADN and HDA (1.4 and $4.6\ s^{-1}$, respectively). Importantly, this sequence is in accord with that of the binding energy of the terminal functional group with the Au electrode (2.4, 0.89, and 0.48 eV for HDT, HDA, and ADN, respectively).[39] Although this relationship might seem to be obvious, it provides important implication for investigating a single-molecule chemical process, including reactions, within the molecular junction. The breakdown of molecular junctions is thermally activated process,[27] which could reduce the effect of the molecular properties,[40] e.g., molecular binding energy, on the observed current or conductance signals. Nevertheless, the relationship between the rate constant of the junction and the binding energy indicates that the desorption of the single molecules governs the breakdown kinetics of single-molecule junctions measured by the *I*–*t* technique. We, therefore, conclude that the analysis of the *I*–*t* traces offers a unique means to reveal the kinetic properties of single-molecule junctions.

The cumulative histograms as shown in Fig. 3 features linear regions at the long survival times, which indicates that a single mechanism dominates the junction breakdown process. However, the histograms deviate from the linearity at the short-time regime (shorter than 0.1–0.2 s). The non-linearity indicates the existence of short-lived single-molecule junctions, in addition to the long-lived, stable ones. We attribute these species to the junctions with metastability. Possible origins can be attributed to unfavourable bonding geometries of the anchoring group to the substrate and/or atomic movements at the electrode surfaces.[39] The metastable molecular junctions are found to be prominent in the 2D histograms in Fig. 2 and smear the presence of the stable junctions. This result underscores the necessity for the kinetic analyses in the argument of the stability of single-molecule junctions.

In summary, the *I*–*t* measurement was utilized to explore the single-molecule junctions having different terminal anchoring groups. The measurement resulted in the observation of the current plateaus arising from the spontaneous formation and breakdown of the molecular junctions. It was found that the lifetime of the junctions depends on the anchoring group of the constituent molecule. The lifetime was successfully analysed to deduce the kinetic properties of the breakdown process of the single-molecule junction, leading to the finding the relation between the rate constant of the junction and the binding energy of the anchoring group. The present research paves the way for the kinetic investigation of a chemical reaction on a single-molecule basis using the molecular junctions.

This work is supported by JSPS KAKENHI Grant Numbers JP16K14018 and JP18H02003.

Conflicts of interest

There are no conflicts to declare.

Notes and references

1. A. B. Zrimsek, N. H. Chiang, M. Mattei, S. Zaleski, M. O. McAnally, C. T. Chapman, A. I. Henry, G. C. Schatz and R. P. Van Duyne, *Chem. Rev.*, 2017, **117**, 7583-7613.
2. S. V. Aradhya and L. Venkataraman, *Nat. Nanotechnol.*, 2013, **8**, 399-410.
3. G. Patterson, M. Davidson, S. Manley and J. Lippincott-Schwartz, *Annu. Rev. Phys. Chem.*, 2010, **61**, 345-367.
4. S. Howorka and Z. Siwy, *Chem. Soc. Rev.*, 2009, **38**, 2360-2384.
5. K. C. Neuman and A. Nagy, *Nat. Methods*, 2008, **5**, 491-505.
6. R. Roy, S. Hohng and T. Ha, *Nat. Methods*, 2008, **5**, 507-516.
7. A. Aviram and M. A. Ratner, *Chem. Phys. Lett.*, 1974, **29**, 277-283.
8. T. A. Su, M. Neupane, M. L. Steigerwald, L. Venkataraman and C. Nuckolls, *Nat. Rev. Mater.*, 2016, **1**, 16002.
9. L. Sun, Y. A. Diaz-Fernandez, T. A. Gschneidtner, F. Westerlund, S. Lara-Avila and K. Moth-Poulsen, *Chem. Soc. Rev.*, 2014, **43**, 7378-7411.
10. A. Coskun, J. M. Spruell, G. Barin, W. R. Dichtel, A. H. Flood, Y. Y. Botros and J. F. Stoddart, *Chem. Soc. Rev.*, 2012, **41**, 4827-4859.
11. E. Evans, *Annu. Rev. Biophys. Biomol. Struct.*, 2001, **30**, 105-128.
12. B. Xu and N. J. Tao, *Science*, 2003, **301**, 1221.
13. D. Xiang, X. L. Wang, C. C. Jia, T. Lee and X. F. Guo, *Chem. Rev.*, 2016, **116**, 4318-4440.
14. D. Xiang, H. Jeong, T. Lee and D. Mayer, *Adv. Mater.*, 2013, **25**, 4845-4867.
15. N. J. Tao, *Nat. Nanotechnol.*, 2006, **1**, 173-181.
16. M. Elbing, R. Ochs, M. Koentopp, M. Fischer, C. von Hänisch, F. Weigend, F. Evers, H. B. Weber and M. Mayor, *Proc. Natl. Acad. Sci. U.S.A.*, 2005, **102**, 8815.
17. I. Díez-Pérez, J. Hihath, Y. Lee, L. Yu, L. Adamska, M. A. Kozhushner, I. I. Oleynik and N. Tao, *Nat. Chem.*, 2009, **1**, 635.
18. C. Guo, K. Wang, E. Zerah-Harush, J. Hamill, B. Wang, Y. Dubi and B. Xu, *Nat. Chem.*, 2016, **8**, 484.
19. D.-H. Chae, J. F. Berry, S. Jung, F. A. Cotton, C. A. Murillo and Z. Yao, *Nano Lett.*, 2006, **6**, 165-168.
20. I. Diez-Perez, Z. Li, J. Hihath, J. Li, C. Zhang, X. Yang, L. Zang, Y. Dai, X. Feng, K. Muellen and N. Tao, *Nat. Commun.*, 2010, **1**, 31.
21. C. Huang, M. Jevric, A. Borges, S. T. Olsen, J. M. Hamill, J.-T. Zheng, Y. Yang, A. Rudnev, M. Baghernejad, P. Broekmann, A. U. Petersen, T. Wandlowski, K. V. Mikkelsen, G. C. Solomon, M. Brøndsted Nielsen and W. Hong, *Nat. Commun.*, 2017, **8**, 15436.
22. L. Meng, N. Xin, C. Hu, J. Wang, B. Gui, J. Shi, C. Wang, C. Shen, G. Zhang, H. Guo, S. Meng and X. Guo, *Nat. Commun.*, 2019, **10**, 1450.
23. W. Haiss, H. van Zalinge, S. J. Higgins, D. Bethell, H. Höbenreich, D. J. Schiffrin and R. J. Nichols, *J. Am. Chem. Soc.*, 2003, **125**, 15294-15295.
24. W. Haiss, R. J. Nichols, H. van Zalinge, S. J. Higgins, D. Bethell and D. J. Schiffrin, *Phys. Chem. Chem. Phys.*, 2004, **6**, 4330-4337.
25. F. Chen, X. Li, J. Hihath, Z. Huang and N. Tao, *J. Am. Chem. Soc.*, 2006, **128**, 15874-15881.
26. Y. S. Park, A. C. Whalley, M. Kamenetska, M. L. Steigerwald, M. S. Hybertsen, C. Nuckolls and L. Venkataraman, *J. Am. Chem. Soc.*, 2007, **129**, 15768-15769.
27. Z. Huang, F. Chen, P. A. Bennett and N. Tao, *J. Am. Chem. Soc.*, 2007, **129**, 13225-13231.
28. M. Tsutsui, K. Shoji, K. Morimoto, M. Taniguchi and T. Kawai, *Appl. Phys. Lett.*, 2008, **92**, 223110.
29. M. Tsutsui, M. Taniguchi and T. Kawai, *J. Am. Chem. Soc.*, 2009, **131**, 10552-10556.
30. M. Kamenetska, M. Koentopp, A. C. Whalley, Y. S. Park, M. L. Steigerwald, C. Nuckolls, M. S. Hybertsen and L. Venkataraman, *Phys. Rev. Lett.*, 2009, **102**, 126803.
31. V. Kaliginedi, P. Moreno-García, H. Valkenier, W. Hong, V. M. García-Suárez, P. Buiter, J. L. H. Otten, J. C. Hummelen, C. J. Lambert and T. Wandlowski, *J. Am. Chem. Soc.*, 2012, **134**, 5262-5275.
32. M. T. González, A. Díaz, E. Leary, R. García, M. Á. Herranz, G. Rubio-Bollinger, N. Martín and N. Agraït, *J. Am. Chem. Soc.*, 2013, **135**, 5420-5426.
33. J. Brunner, M. T. González, C. Schönenberger and M. Calame, *J. Phys.: Condens. Matter*, 2014, **26**, 474202.
34. D. Xiang, V. Sydoruk, S. Vitusevich, M. V. Petrychuk, A. Offenhäusser, V. A. Kochelap, A. E. Belyaev and D. Mayer, *Appl. Phys. Lett.*, 2015, **106**, 063702.
35. T. Harashima, Y. Hasegawa, S. Kaneko, M. Kiguchi, T. Ono and T. Nishino, *Angew. Chem. Int. Ed.*, 2019, **58**, 9109-9113.
36. W. Lee and P. Reddy, *Nanotechnology*, 2011, **22**, 485703.
37. R. Frisenda, S. Tarkuç, E. Galán, M. L. Perrin, R. Eelkema, F. C. Grozema and H. S. J. van der Zant, *Beilstein J. Nanotechnol.*, 2015, **6**, 1558-1567.
38. C. R. Peiris, Y. B. Vogel, A. P. Le Brun, A. C. Aragonès, M. L. Coote, I. Díez-Pérez, S. Ciampi and N. Darwish, *J. Am. Chem. Soc.*, 2019, **141**, 14788-14797.
39. W. Hong, D. Z. Manrique, P. Moreno-García, M. Gulcur, A. Mishchenko, C. J. Lambert, M. R. Bryce and T. Wandlowski, *J. Am. Chem. Soc.*, 2012, **134**, 2292-2304.
40. C. Bruot, J. Hihath and N. Tao, *Nat. Nanotechnol.*, 2011, **7**, 35.

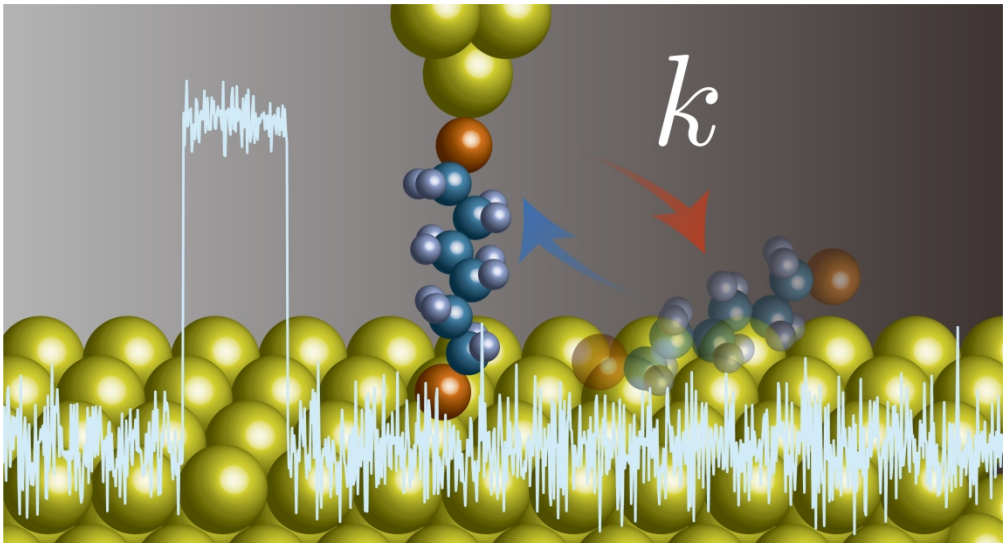

207x112mm (300 x 300 DPI)